EXPERIMENTAL DETERMINATION OF THE MULTI-AXIAL STRAIN TRANSFER FROM CFRP-LAMINATES TO EMBEDDED BRAGG SENSOR

KEYWORDS

Structural health-monitoring, optical fibre sensor, Bragg grating, embedded sensors, strain transfer, composite materials

INTRODUCTION

Superior design flexibility and fatigue performance render composite materials attractive successors for traditional construction materials. However, due to their anisotropic nature, isotropic material design procedures are no longer valid. Additionally, more complex strain distributions and failure modes exist. Therefore, internal strain information can provide useful knowledge concerning composite behavior both in material characterization and online health monitoring (e.g. smart structures). Embedding optical fibre Bragg gratings can even provide multi- axial strain information. Determining the total strain field in composite structures is of upmost importance, since they render valuable information on the integrity of the structure.

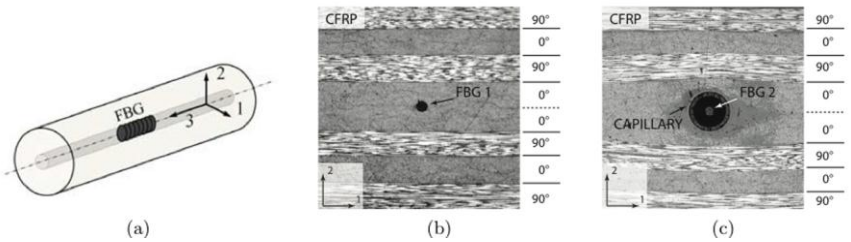

Figure 1: (a) The coordinate system used for all equations in this paper. (b) & (c) The cross-sections of a dual- FBG configuration inside a cross-ply composite material (b) the first FBG, (c) the second FBG en-capsulated inside a capillary

In (Luyckx et al. 2010a), the usability of 80µm draw-tower gratings (DTG® (Rothard et al. 2004)) embedded in carbon fibre reinforced composite is explored as a multi-axial strain sensor. DTGs are optical fibres in which the grating is inscribed during the drawing process with a single laser pulse. The response of such DTGs is, like any other FBG, dictated by Bragg's law. Using a small-strain approximation and the centre strain theory (valid for conventional fibres), the temperature and strain sensitivity of an FBG along its polarization axes can be written as (Lawrence et al. 1999):

$$\frac{\Delta\lambda_{B,1}}{\lambda_B} = \varepsilon_3 - \frac{\bar{n}^2}{2}[p_{11}\varepsilon_1 + p_{12}(\varepsilon_2 + \varepsilon_3)] + \beta\Delta T \qquad (1)$$

$$\frac{\Delta\lambda_{B,2}}{\lambda_B} = \varepsilon_3 - \frac{\bar{n}^2}{2}[p_{11}\varepsilon_2 + p_{12}(\varepsilon_1 + \varepsilon_3)] + \beta\Delta T \quad (2)$$

in which p_{11} and p_{12} are the strain optic coefficients. The coordinate system is as depicted in Figure 1(a). The 1- and 2-axis are oriented according to the optical slow and fast axis. These will align with the principal directions of transverse strain. Using a dual-FBG configuration (Figure 1(b)-(c)), in which both FBGs are exposed differently to the strain field, equations (1)-(2) can be inverted to yield the strain-field from the measured wavelength shifts. In (Luyckx et al. 2010a) and this paper, the second FBG is encapsulated in a capillary tube (Figure 1(c)), which isolates it from transverse stresses. As such, ε_1 and ε_2 are equal to $-\nu\varepsilon_3$, resulting in an equal shift of both wavelengths for this FBG. Temperature-compensation is achieved using an external sensor. The matrix-formalism yielding the principal strains from the measured wavelength shifts in this configuration can be written as:

$$\begin{bmatrix} -\frac{\bar{n}^2}{2}p_{11} & -\frac{\bar{n}^2}{2}p_{12} & 1-\frac{\bar{n}^2}{2}p_{12} \\ -\frac{\bar{n}^2}{2}p_{12} & -\frac{\bar{n}^2}{2}p_{11} & 1--\frac{\bar{n}^2}{2}p_{12} \\ 0 & 0 & \left(1--\frac{\bar{n}^2}{2}p_{12}\right)+\upsilon_f\frac{\bar{n}^2}{2}(p_{11}+p_{12}) \end{bmatrix}^{-1} \begin{bmatrix} \Delta\lambda_{B,1,a}/\lambda_{B,a} \\ \Delta\lambda_{B,2,a}/\lambda_{B,a} \\ \Delta\lambda_{B,b}/\lambda_{B,b} \end{bmatrix} = \begin{bmatrix} \varepsilon_1 \\ \varepsilon_2 \\ \varepsilon_3 \end{bmatrix} \quad (3)$$

with ν_f , the poisson-coefficient of the optical fibre. The matrix relating wavelength-shifts and strains is called the K-matrix.

STRAIN TRANSFER

The optical fibre can be regarded as an inclusion inside the material (Fig. 1(b,c)). Because mechanical strains and stresses will be redistributed in the vicinity of the optical fibre, the mismatch in material properties between the composite and the optical fibre has to be taken into account (Fig. 2). As a result, the strains deduced from equations (1)-(2), which represent those measured at the center of the optical fibre core, will differ from the actual strains that would exist in the undisturbed composite. When strain-gradients are limited, the strains that would occur in an undisturbed structure will be equal to the strains at a certain distance from the fibre. The multi-axial transfer of strain from the composite (e.g. the actual strains) to the fibre core (e.g. measured strains) was modeled in (Luyckx et al. 2010b) It was shown that axial strain transfer is usually in the vicinity of 100%, while transverse strain transfer is

dependent on many parameters such as ply lay-up and material properties (Luyckx et al. 2010b).

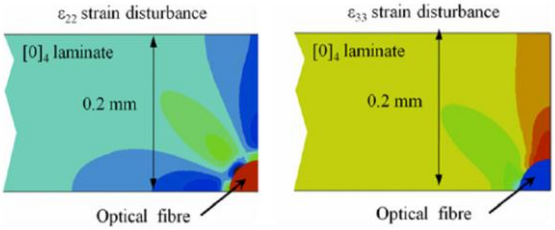

Figure 2: Transverse strain disturbance for a thin laminate [0]4 loaded in the transverse out-of-plane direction. The optical fibre sensor is embedded in the middle of the laminate. (Luyckx et al. 2010b)

In (Luyckx et al. 2010b), a general method of modeling the strain transfer using matrix formalism is proposed:

$$[\varepsilon^c] = [TC][\varepsilon^s] \tag{4}$$

where ε^s symbolizes the sensed strains, and ε^c the composite strains, TC is called the multi-axial strain transfer matrix. Using numerical simulations, the TC-matrix has been calculated for the case of $[0_2, 90_2]_{2s}$ cross- ply carbon-fibre reinforced thermosetting polymer (CFRP) laminates with embedded 80µm optical fibres. The TC-matrix was found to be (The matrix was transformed to match the coordinate system in this paper (Fig. 1)):

$$TC_{[0_2,90_2]_{2s}} = \begin{bmatrix} 7{,}64 & -1{,}23 & 0{,}82 \\ -1{,}24 & 7{,}62 & 0{,}81 \\ 0 & 0 & 1 \end{bmatrix} \tag{5}$$

Equation (4) can be extended with the aforementioned K-matrix, leading to a direct correlation between composite strains and wavelength shift:

$$[\varepsilon^c] = [TC][K]^{-1}\left[\Delta\lambda/\lambda\right] \tag{6}$$

EXPERIMENTAL RESULTS

Using equation (6), the numerical TC-matrix has been validated experimentally. Different CFRP samples with $[0_2,90_2]_{2s}$ lay-up were created according to Figure 3.

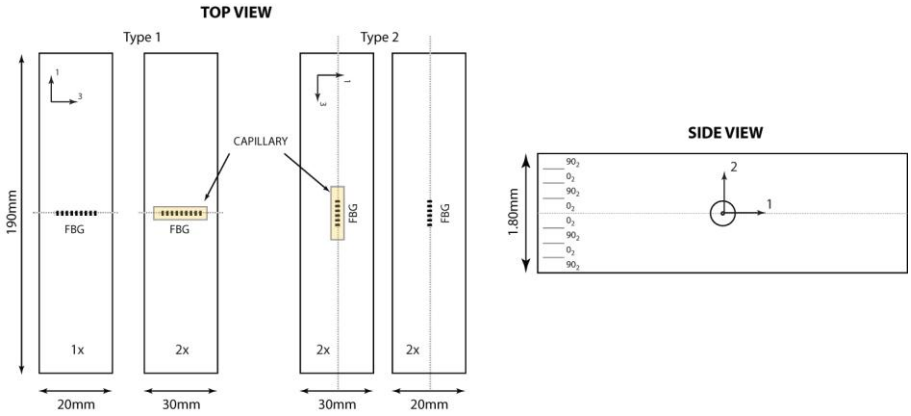

Figure 3: Dimension and lay-out of experimental samples.

According to (Luyckx et al. 2010b) 3 different loading conditions are required to determine the TC-matrix. Both tensile loading in the length direction (1-direction for Type 1, 3-direction for Type 2) according to the ASTM D3039 standard and through-the-thickness compression loading (2 direction) were performed. All tests were performed three times. The wavelength shifts for the different loading conditions were recorded for the different samples (Fig. 4). The results show an almost perfect linear behavior for loading along the 2-direction and 3-direction. Significantly more scattering is visible on the wavelength response of the capillary Type-1 sample (black squares in Fig. 4(a)). In the future, more samples will be created to better study the behavior of this sample-type. These wavelength shifts are then translated to sensor strains (ε^s) using the K-matrix by substituting $\nu_f = 0.17$, $n = 1.456$, $p_{11} = 0.111$ and $p_{12} = 0.247$ in equation (3).

The composite strains ε^c are determined using finite element simulations, for which the material properties have been determined previously. Using the three different strain fields ε^c and ε^s – corresponding to the three distinct loading conditions –, the TC-coefficients can be found from equation (4).

$$TC_{[0_2,90_2]_{2s}} = \begin{bmatrix} 7{,}49 & -2{,}01 & 0{,}69 \\ -2{,}45 & 7{,}87 & 0{,}77 \\ -0{,}01 & -0{,}01 & 0{,}96 \end{bmatrix} \quad (7)$$

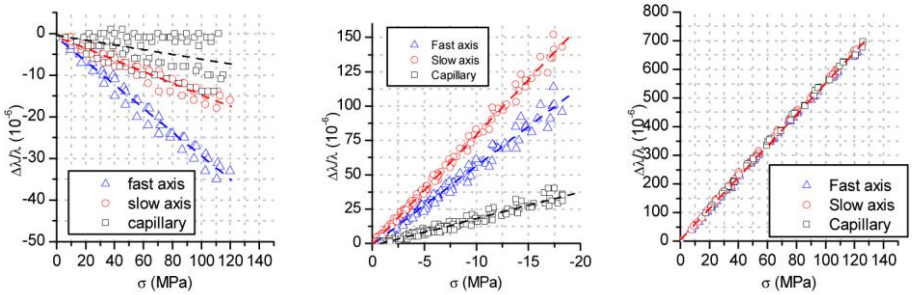

Figure 4: Wavelength shifts for loading in the (a) 1-direction, (b) 2-direction and (c) 3-direction.

If one compares equation (7) to equation (5), a more than decent correspondence between experiment and simulation has been found. Both matrices clearly show almost perfect axial strain transfer. In contrast, only part of the transverse strains are transferred, and both matrices show a significant cross-sensitivity to transverse strains. This cross-sensitivity is higher for the experimental matrix, than for the numerical matrix. This could be caused by the large spread in the response of the capillary Type-1 sample. The good correspondence can be further validated and refined using additional testing.

CONCLUSIONS

Despite the manual lay-up procedure for the experimental samples, it is clear that there is a strong correspondence between experimental (7) and numerical (5) TC-matrix. This entails that numerical simulations can be used to determine the TC-matrix for more complex structures. Additionally, it is clearly illustrated that the proposed experimental set-up is capable of accurately determining the strain transfer. Finally, the experimentally and numerically determined TC-matrix shows the importance of translating the measured strains to the actual strains, which can significantly differ from each other.

INDUSTRIAL PARTNER

The author is funded by a EU FP7 project called SMARTFIBER. Therefore, the authors like to acknowledge the European Union and their partners IMEC, Airborne Technology Centre, FBGS Technologies, Xenics, Fraunhofer IIS and Optocap.

CONTACT

N. Lammens
Department of Materials Science & Engineering – UGent

Nicolas.Lammens@ugent.be

REFERENCES

Rothhardt, M., Chojetzki, C., and Mueller, H. R., *"High mechanical strength single-pulse draw tower gratings,"* Int. Conf. on Applications of Photonics Technology (Ottawa) (2004).

Lawrence, C., Nelson, D., Udd, E., and Bennett, T., *"A fiber optic sensor for transverse strain measurement,"* Experimental Mechanics 39(3), 202–209 (1999).

Luyckx, G., Voet, E., Lammens, N., De Waele, W., and Degrieck, J., *"Multi-axial strain transfer from laminated CFRP composites to embedded Bragg sensor,"* Proceedings OFS21 (Canada) (2010).

Luyckx, G., Voet, E., De Waele, W., and Degrieck, J., *"Multi-axial strain transfer from laminated CFRP composites to embedded Bragg sensor: I. Parametric study,"* Smart Materials and Structures (2010).